

PAPER

ResFCNET: A Skin Lesion Segmentation Method Based on a Deep Residual Fully Convolutional Neural Network

Mustapha Adamu
Mohammed^{1,2}(✉), Obeng
Bismark³, Seth Aloroyo¹,
Michael Asante², Bernard
Obo Essah⁴

¹Department of Computer Science, Koforidua Technical University, Koforidua, Ghana

²Department of Computer Science, Kwame Nkrumah University of Science and Technology, Kumasi, Ghana

³School of Computer and Information Engineering, Zhejiang Gongshang University, Hangzhou, People's Republic of China

⁴Department of Statistics & Actuarial Science, University of Ghana, Legon-Accra, Ghana

adamu.mohammed@ktu.edu.gh

ABSTRACT

Melanoma, a high-level variant of skin cancer, is very difficult to distinguish from other skin cancer types in patients. The presence of a large variety of sizes of lesions, fuzzy boundaries, their irregular-shaped nature, and low contrast between skin lesions and surrounding flesh areas make it clinically difficult to detect and treat melanoma. In this paper, we propose Residual Full Convolutional Network (ResFCNET), a skin lesion recognition model that combines residual learning and a full convolutional network to perform semantic segmentation of skin lesion. Based on secondary-feature extraction and classification, an experiment was done to verify the effectiveness of our model using the ISBI 2016 and ISBI 2017 dataset. Results showed that a residual convolution neural network obtained high-precision classification. This technique is novel and provides a compelling insight for medical image segmentation.

KEYWORDS

deep learning, fully convolutional network, image segmentation, melanoma, residual learning

1 INTRODUCTION

Melanoma is rare but the deadliest among all skin cancer types [1]. This type of cancer of the skin is caused by the exposure of the human skin to excessive sun rays. According to available data, the United States, New Zealand, and Australia have the world's highest rates of skin cancer, accounting for 75% of all skin cancer-related deaths [2], [3]. If detected and treated at the early stages, the chances of patients being cured are high. Conversely, melanoma has the tendency to spread to neighboring parts of the affected region of the body; then, treatment becomes a near impossibility and this results in death. Therefore, segmenting, or delineating the boundary of, melanoma lesions is vital intervention in reducing the rate of spread and promoting a timely cure. [4].

Mohammed, M.A., Bismark, O., Aloroyo, S., Asante, M., Essah, B.O. (2023). ResFCNET: A Skin Lesion Segmentation Method Based on a Deep Residual Fully Convolutional Neural Network. *IETI Transactions on Data Analysis and Forecasting (iTDAF)*, 1(1), pp. 4–19. <https://doi.org/10.3991/itdaf.v1i1.35723>

Article submitted 2022-09-30. Resubmitted 2023-02-10. Final acceptance 2023-02-13. Final version published as submitted by the authors.

© 2023 by the authors of this article. Published under CC-BY.

Malignant melanoma has been on the rise in various parts of the world in recent times [5], with a high mortality rate, with nearly 76,380 cases recorded annually and 10,130 deaths reported in the United States alone. The increasing rise in climate change in recent years is expected to result in a further increase in instances in many parts of the world [6]. Even though there are modern treatment methods such as radiation therapy, chemotherapy, and surgery in practice [7], classifying and diagnosing melanoma skin cancer remains the main challenge [6], [8]. Early identification is critical to the patient's survival, which is five years and with only a 15% survival probability in most melanoma cases that have progressed, whereas patients with melanoma diagnosed in its early stages have a 75% survival rate. This variation in percentages demonstrates that identifying melanoma at the early stages is vital in timely diagnosis and early treatment. In most cases, skin disease specialists have employed pathology for the confirmation of skin lesions [9]. This method can sometimes be time consuming and delay the process of detecting the disease. In other cases, dermatologists rely on expert consensus for the confirmation of skin lesions. Again, this approach can be inaccurate and susceptible to errors, even in the hands of an experienced dermatologist.

In recent times, machine learning methods have provided viable alternatives that have improved the detection of benign and malignant skin lesions [10]. New extraction methods feature using Support Vector Machine Random Forest, K-Nearest Neighbor, and Naïve Bayes classifiers to classify skin cancer as melanoma or benign lesions [11]. For image segmentation, this model achieved a Dice coefficient of 77.5% and an SVM classifier accuracy of 85.19%.

Akram, Khan, Sharif, & Yasmin focused on improving segmentation and feature selection of dermoscopic images using a multilevel support vector machine [12]. A new feature extraction and dimensionality reduction criterion was designed that incorporates both traditional and new feature extraction strategies. The suggested method is assessed using many criteria such as FPR, sensitivity, specificity, FNR, and accuracy using the PH2, ISBI 2016, and ISIC benchmark data sets. The statistics show that the proposed strategy outperforms a number of existing strategies by a significant margin.

Machine learning models adopt manual feature selection and feature extraction with traditional tree-based algorithms such as decision trees, support vector machine (SVM), and cluster-based algorithms such as K-Nearest Neighbor to realize the classification and segmentation of skin cancers. This manual feature engineering approach can come in handy if the data is not too huge. However, with increasing amounts of data, machine learning approaches can become ineffective. Again, training of machine learning algorithms for automated classification of skin lesions is hampered by the small size of images and the difficulty in understanding images with different features. The recent success of deep learning for object detection and classification problems has generated insight in applying the methods to semantic segmentation. Deep learning approaches employ end-to-end training procedure, which automatically extract features without relying on a manual features engineering process.

The researchers in Long [13], deployed a fully convolutional network to perform pixel-wise segmentation. The authors adapted Google Net classification technique for their classification task as the convolutional layers were replaced with a fully connected layer. As an extension of the work of Long [13], Hong et al. [14] proposed a deconvolutional network, which decoupled the classification task through the

adoption of bridging layers to design new feature maps that could reduce training time. In spite of the successes achieved [13], [14], the fully convolutional models used pooling layers that sought to reduce the dimensionality of the image data. This leads to loss of vital information. However, there is the need to preserve exact information of class maps to achieve semantic segmentation.

Kolekar & Magdum proposed pixel-wise semantic segmentation of skin lesions using a convolutional encoder-decoder neural network [15]. The authors trained and tested their model on the same dataset used in this paper. Experimental results of their approach achieved a Jaccard index value of 92.8%. Even though the encoder-decoder networks work efficiently in keeping the output image resolution, the network becomes deeper and slow to train.

Kaur et al. [16] proposed an end-to-end atrous spatial pyramid pooling-based convolutional neural network for automatic lesion segmentation. Based on the concept of atrous dilated convolutions, the authors constructed a model and tested it on the ISBS 2016, 2017, and 2018 datasets. Their model achieved a Jaccard index of 86.5% on ISBS 2016, 81.2% on ISBS 2017, and 81.2% on ISBS 2018 datasets, respectively.

This study aims to further the development of effective models for automated diagnosis of melanoma, which is among the deadliest types of skin cancer along with squamous and nevus, according to [17]. Therefore, we introduce an enhanced fully convolutional network (FCN)-based deep network for skin lesion segmentation (ResFCNET). The design is composed of an encoder and a decoder. The encoder transforms an image into a representation. Semantic segmentation is then performed by the decoder, which recovers the representation. The encoding portion comprises five residual units with 3×3 convolutional blocks combined with an identity map. The residual blocks assist the network to learn features from previous levels, and high-semantic features from deeper layers. Each convolutional block is composed of a 3×3 convolutional layer with each normalization and Relu activation function.

First, we applied a stride of 2 to reduce sample size of the image instead of using a pooling operation. The images were reduced in size by half, and the identity map connected the unit's input and output. The operation was repeated five times for each residual unit. The decoder path has four residual blocks with each layer starting up with up sampling layer. This allowed the network to learn at a lower level and combine the feature maps from the encoding path with the feature map from the associated encoding path. The last part has convolutional and sigmoid activation where the network can project the multichannel functionality into the desired segmentation. Finally, the proposed model was used for secondary feature extraction, and a classification experiment was conducted. Accuracy, Dice loss sensitivity, and other evaluation metrics were used to evaluate the performance of our model.

2 LITERATURE REVIEW

Deep neural network creation and widespread use have generated a lot of curiosity, opened up a wide range of possibilities for clinical research, and stimulated more studies on risk assessment and disease detection through deep learning. Most of the existing approaches can be classified into supervised fully automatic, semi-automatic, and unsupervised fully automatic. The supervised approach basically extracts region or pixel features like the pixel-level Gaussian features [18], [19] and texture features [20], [21]. It uses several classifiers such as a wavelet network [20],

Bayes classifiers, or support vector machines [21] to differentiate healthy skin from a lesion. The semi-automatic method requires the initialization of the segmentation process by the user or initialization such as the seed-selection method [22] or through contour placement [23]. Then these contours and seed will gradually grow or transform to form skin lesion boundaries based on a function that has been predefined. But this approach has some drawbacks because manual initialization is often time inefficient or it requires a longer time for this process and is subjective and not reproducible. As such, this method is unreliable in the clinical medical environment and is not widely used. The unsupervised fully automatic method mostly depends on thresholding [22], [24], [25], statistical regions merging, and energy functions. Thresholding approaches try to differentiate the skin lesion based on a threshold value, which is usually derived by analyzing image features that have been predefined. These approaches, which rely on energy functions, attempt to identify skin lesion boundaries through minimization of a predefined cost function on the features of images, such as smoothness, statistical distributions, and edges. The second method, statistical region merging, works by iteratively merging regions of pixels in an orderly fashion. Lately, some approaches such as multiscale pixel or region with cellular automata (MSCA) [26], [27] sparse coding with dynamic rule-based refinement (SCDRR) [28] have been used to divide cutaneous lesions. Unsupervised approaches, on the other hand, have the drawback of being unable to appropriately segment difficult skin lesions, such as those with artifacts close by or those that touch the image's multiple boundaries. The thresholding also has some drawbacks; which includes distribution intensity in the skin lesion, which may fail if the distribution has several peaks or highs. All these methods rely on a feature that is low level, such as texture and color features, which cannot accurately capture the variations of a wide image. The unsupervised fully automatic method mostly depends on threshold [22], [24], [25], statistical regions merging, and energy functions. Thresholding approaches try to differentiate the skin lesion based on a threshold value, which is usually derived by analyzing image features that are predefined. These approaches rely on energy functions to try to identify skin lesion boundaries through minimization of a predefined cost function on the features of images such as smoothness, statistical distributions, and edges. The statistical regions merging method is based on recursively merging region of pixels in an orderly manner. Lately, some approaches such as multiscale pixel or region with cellular automata [26], [27] sparse coding with dynamic rule-based refinement (SCDRR) [28] and have been applied to skin lesion segmentation. But unsupervised methods have some disadvantages. For example, they cannot correctly segment some challenging skin lesions, such as a lesion that has artifacts close to it or a lesion that touches the various edges of the image. Thresholding also has some drawbacks, including distribution intensity in the skin lesion, which may fail if the distribution has several peaks or highs. All of the solutions presented rely on low-level properties, such as texture and color, which are incapable of effectively capturing wide-image fluctuations.

Furthermore, these approaches' performances rely mostly on the tuning of large parameters and efficient preprocessing approaches, such as hair removal and correction of illumination. This makes it difficult to apply the method to new images. However, with the rise in artificial intelligence methods, such as machine learning and deep learning, significant headway has been achieved. Convolutional networks are becoming the de facto technique for addressing applied computer vision problems. This section provides an overview of some deep learning methods [13], [29].

Convolutional neural networks (CNNs) have recently achieved notable results in medical image problems, such as body part recognition from computed tomography (CT) images [30], mitosis detection on histology images Cirşan [31], cerebral microbeads detection on magnetic resonance (MR) images [32], 2D/3D image registration [33], and skin cancer classification [34]. CNN has been used to analyze MR images of a brain tumor [35], and CT urography to analyze images of a urinary bladder [30] and nondermoscopic images of a skin lesion, among others. Researchers have developed fully convolutional networks (FCNs) based on this success of [36], [37]. These networks perform a backward stride of the convolution process, normally called deconvolution. These generate maps of the segmented images. Two selected examples are U-net and deconvolution layers.

The availability of enormous datasets, improved algorithms, and processing power have all contributed to the recent explosion in deep learning. This has enabled researchers and practitioners to use deep learning approaches on a variety of medical problems. Object identification, segmentation, and image classification are just a few of the tasks that convolutional neural networks have excelled in [34], [35]. This excellent result can be attributed to the fact that CNNs are capable of learning image feature representations that carry semantic meaning at a high level [38]. LeCun, Bengio, & Hinton recently used a 50-layer-deep residual network to perform segmentation [39]. Yu et al. [40] reported a residual network that was utilized to expand the network's depth. CNN has also shown promising results in the area of medical imaging. Such tasks include mitosis detection on historical images [31] skin cancer classification [34], skin lesion extraction from nondermoscopic images [41], and 2D/3D image registration, urinary bladder segmentation in CT urography [30], among others.

3 METHODOLOGY

3.1 Dataset

The dataset used for this study is the ISBI data called Melanoma detection dataset, available at <https://www.kaggle.com/wanderdust/melanoma-detection>. This is benchmark data provided by International Skin Imaging Collaboration (ISIC) for research on skin cancer and has been used in previous studies such as [16], [42], [43], [44]. Specifically, this study made use of ISBI 2016, and ISBI 2017 thermoscopic image datasets.

Table 1. Dataset distribution for our study

Year	Data Source	Number of Trainings Set	Number of Tests Set	SizeImage
2017	ISBI	2000	600	771×750–6748×4499
2016	ISBI	900	379	1022×787–4288×2848

To accomplish skin lesion segmentation, we proposed a fully convolutional network (FCN), shown in Figure 1. Our model design is made up of two parts: an encoder and a decoder. The encoder transforms an image into a representation. The semantic segmentation is then performed by the decoder portion, which

recovers the representation. The encoding part consists of five residual unit with a 3×3 convolutional block and an identity map. These residual He blocks aid the network in learning features from previous levels as well as high-semantic features from deeper layers [45]. The general shape of the residual block is shown in Equation 1. Each convolutional block is made up of a 3×3 convolutional layer, batch normalization, and the ReLU activation function. Here we applied a stride of 2 instead of using pooling operations to downsample the images. The images are reduced in size by half, and the identity map connects the unit's input and output. For each residual unit, the operation is repeated five times.

$$y_i = h(x_i) + F(x_i W_i) X_{i+1} = f(y_i) \quad (1)$$

$F(\cdot)$ is the residual function, $f(y_i)$ is activation function, and $h(x_i)$ is an identity-mapping function. A typical one is $h(x_i) = x_i$, where $x_i + 1$ denotes the input and output of the i th block.

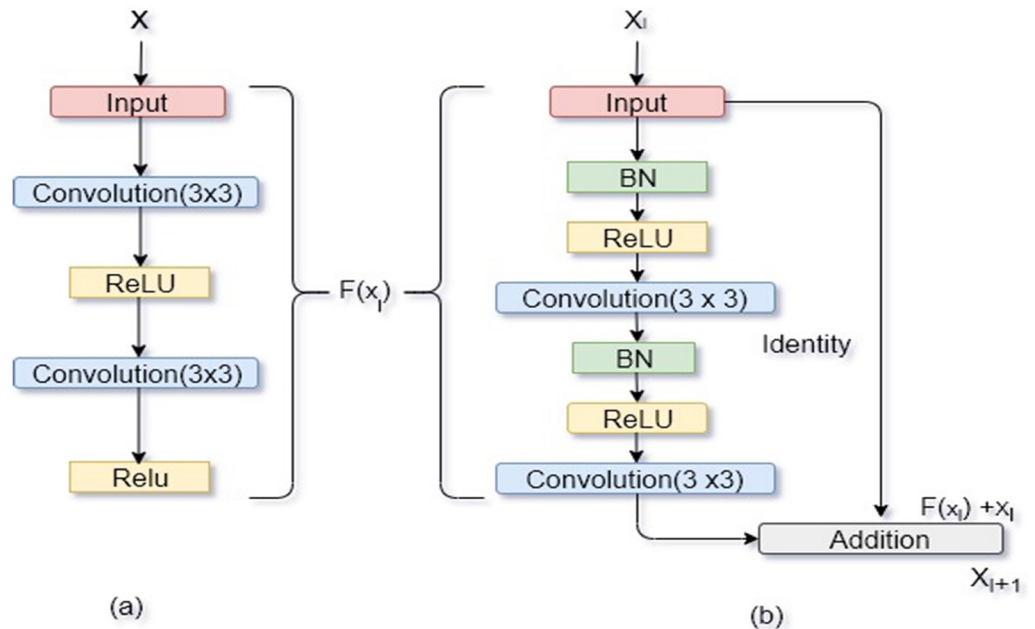


Fig. 1. The difference between a plain convolutional and residual network

The decoder path has four residual blocks, with each layer starting with an upsampling layer. This allows the network to learn at a lower level and concatenate the feature maps from the encoding path with the feature maps from the associated encoding path. The last part of the network has a 1×1 convolutional and sigmoid activation function where the network can then project the multichannel functionality into the required segmentation. The network comprises a total of 20 convolutional layers. Figure 2 shows the outcome of our proposed design in detail and also depicts our suggested architecture.

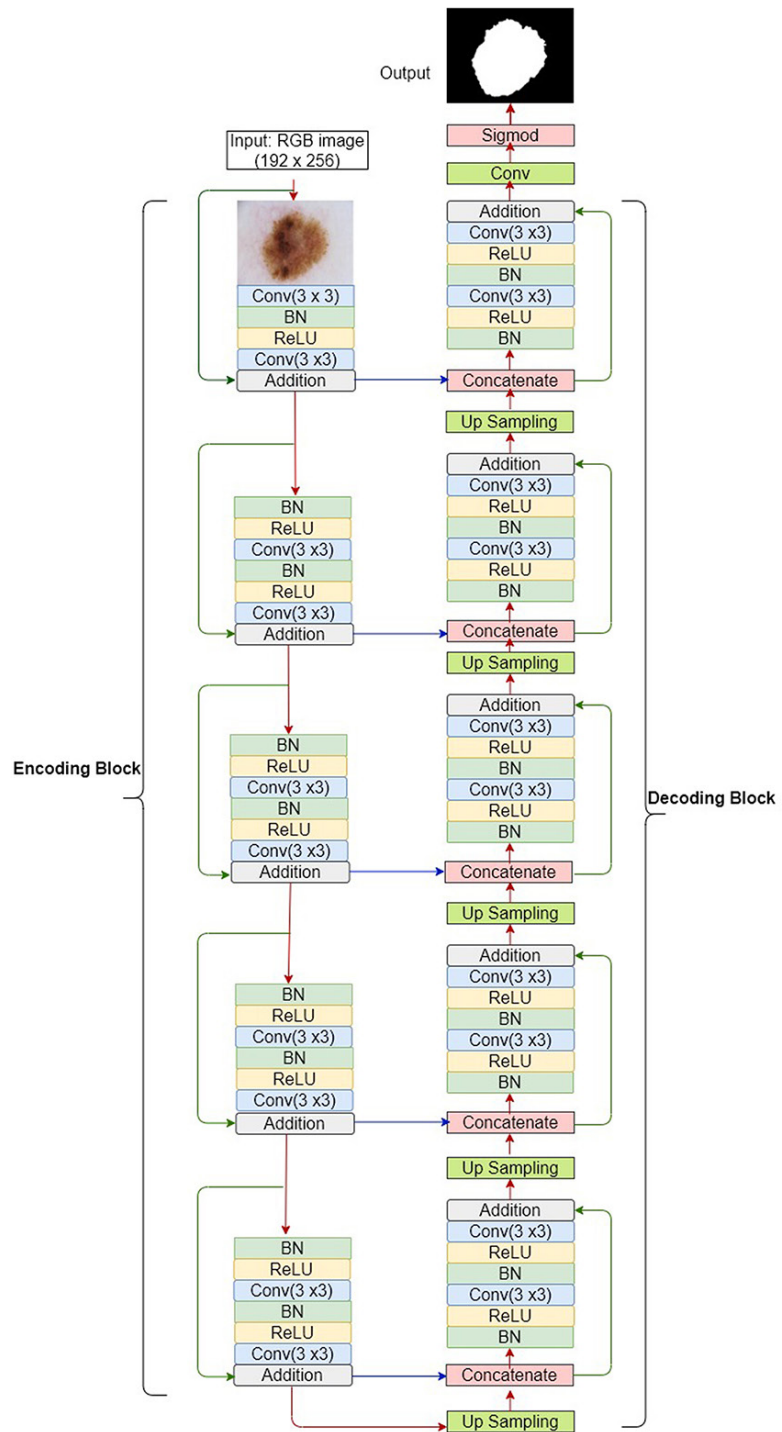


Fig. 2. The encoder and decoder of ResFCNET

The encoder and decoder of ResFCNET are each made up of five blocks. The red arrows indicate network connectivity, the green arrows indicate the identification block, and the blue arrows indicate skip connections.

3.2 Experiments and performance metrics

Experimental environment. The simulation experiments were performed on a physical machine running on 1.4 GHz Quad-Core Intel Core i5, with 8 GB 2133 MHz LPDDR3 memory and macOS Monterey version 12.3 64-bit operating system.

Our model was built with Keras [46] and TensorFlow [47], and trained with a resized image of 192×256 RGB images. The image was normalized to obtain the pixel value between 0 and 1. We flipped the image vertically with a probability of 0.5 and again flipped it at another probability of 0.5. The next step was to apply a rotation at an angle of theta, which was randomly sampled by using a Gaussian distribution with the range of [−400, 400]. The weights of the network were initialized using Xavier initialization [48] and trained using a stochastic gradient descent [49] while minimizing Equation 2, with an Adam optimizer [50], learning rate of 10^{−4}. The network was trained on Tesla K40 GPU with 12 GB GDDR5.

Evaluation metrics. Accuracy (AC), Dice loss (DI), sensitivity (SE), specificity (SP), and Jaccard coefficient (JC) were adopted in this study to evaluate the performance of our proposed model, defined as follows:

$$AC = \frac{(TP + TN)}{(TP + FP + FN)} \quad (2)$$

$$DI = \frac{(TP + TN)}{(2 \times TP + FP + FN)} \quad (3)$$

$$SE = \frac{(TP)}{(TP + FN)} \quad (4)$$

$$SP = \frac{(TN)}{(TN + FP)} \quad (5)$$

$$JC = \frac{(TP)}{(TP + FP + FN)} \quad (6)$$

where TP , TN , FP , and FN denote the number of true positives, true negatives, false positives, and false negatives, respectively.

Experiments on ISBI 2016 and ISBI 2017 skin lesion datasets. The 2016 datasets contained 1279 RGB images. The image was divided into 900 training annotated dermoscopic images with 727 benign images and 173 melanomas. It also had a 379-validation set with 75 melanomas and 304 benign. This was 8-bit RGB images with sizes ranging from 542×718 to 2848×4288. The 2017 dataset had 2000 training with a test sample of 600. The sizes of the images ranged from 771×750 to 6748×4499.

4 RESULTS AND ANALYSIS

Using three distinct image sizes, we compared the segmentation performance: 96×128, 192×256, and 384×512. The Dice coefficient improved from 0.937 to 0.938 when the image size was increased from 96×128 to 192×256, but it dropped to 0.873 when the image size was increased to 384×512, as shown in Table 2. The quadrupled quantity of pixels made model training more difficult, which resulted in a

performance drop. Although expanding model capacity by adding more layers or features may increase performance for 384×512 images, it would be extremely time consuming. At the moment, 384×512 epoch training takes 110 seconds, 192×256 takes 27 seconds, and 96×128 takes 8 seconds. These findings suggest that a 192×256 image size provides a fair mix of segmentation performance and computing cost; thus, we downsized all of the images to this resolution before putting them into the ResFCNET model. The results with different size of images are shown in Table 2. Our model increased segmentation performance in terms of Dice similarity and Jaccard coefficient.

Table 2. Results of different input size

Input Size	AC	DC	JC	SE	SP
98×128	0.974	0.937	0.856	0.920	0.994
192×256	0.970	0.938	0.865	0.9189	0.989
284×512	0.941	0.873	0.861	0.920	0.972

4.1 Behavior of training epochs, accuracy, and loss function

A loss function measures the performance of a classification model whose output is a probability value between 0 and 1 and is known as cross-entropy loss. This pixel-wise classification may favor the background image above the lesions, resulting in the lesion not being effectively segmented or missing. A solution to this problem would be to give each pixel a weight during the training process that will compensate the gaps in frequencies of pixels from each class. So to help re-balance the contribution of both the background and the lesion areas, various methods have been proposed. Although these devised loss approaches help in balancing the class [43], they come with additional computational cost during the training process. The Jaccard index [43] shown in Equation 2 was adopted:

$$L_j = \frac{\sum_{ij} (t_{ij} p_{ij})}{\sum_{ij} t_{ij}^2 + \sum_{ij} p_{ij}^2 - \sum_{ij} t_{ij} p_{ij}} \tag{7}$$

The size of the intersection divided by the size of the union of the sample sets is a formal definition of the measurement, which stresses similarity between finite sample sets. It takes into consideration both missed values and false alarms in all the classes. This helps in addressing medical images with high-class imbalance. Figure 3 shows training loss and validation loss output achieved during the training (epochs). The graph shows that the validation loss fluctuates at different complete passes of our training set through the algorithm. The epoch is an important parameter for the algorithm to train our model, as the accuracy and validation loss values are obtained at the end of every epoch. We aim at obtaining the model that has the lowest validation loss. However, we can have thousands of epochs running, but we set a stopping point when we have a minimal model error. This is taken as the best model to fit our dataset well. Figure 4 indicates the accuracy characteristics obtained during different epochs.

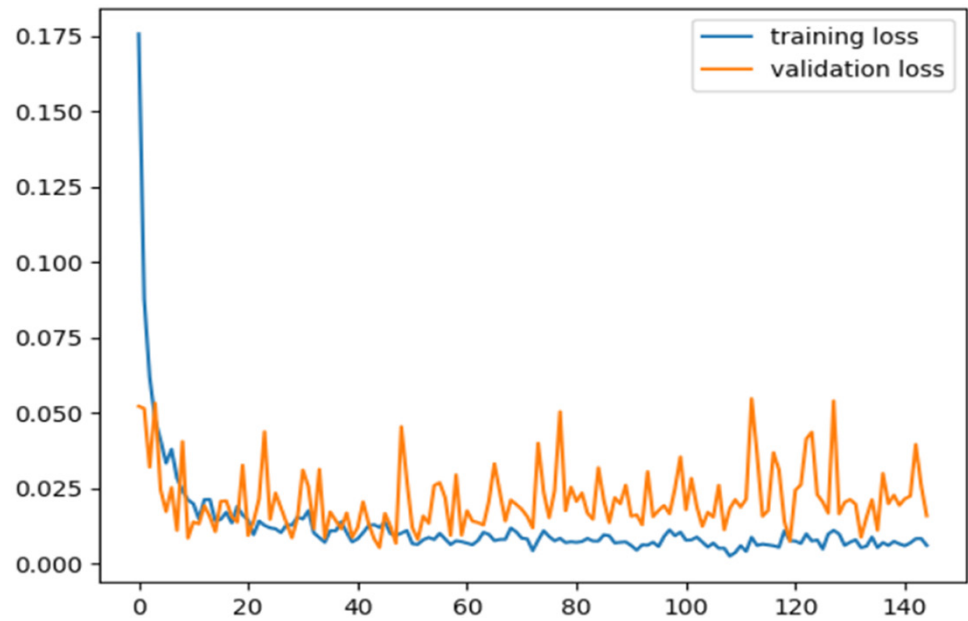


Fig. 3. Training loss and validation loss obtained at different epochs

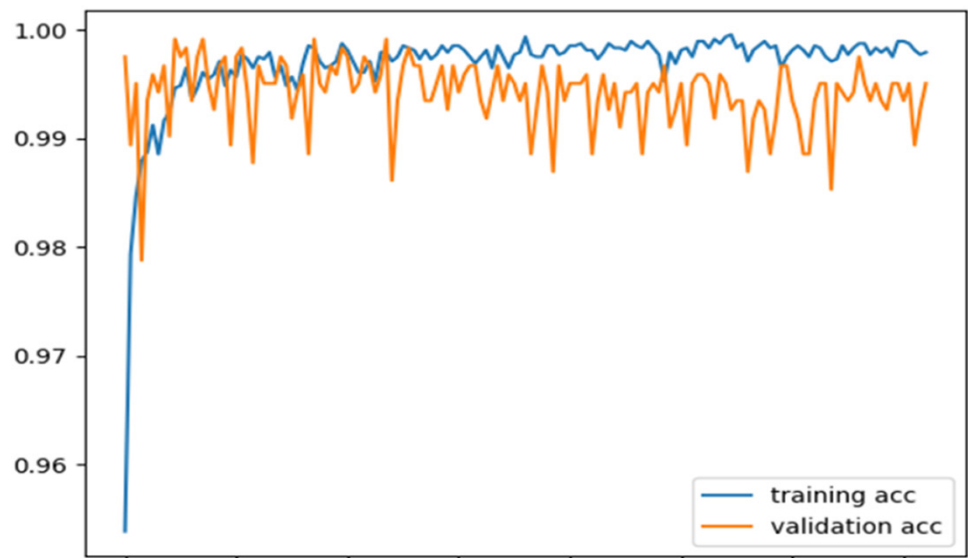


Fig. 4. Accuracies obtained for training and validation at different epochs

Table 3. Results of different loss functions

Loss Function	AC	DC	JC	SE	SP
Jaccard index	0.971	0.942	0.866	0.925	0.989
Cross entropy	0.970	0.938	0.865	0.9189	0.959

Because of the class imbalances, cross-entropy loss is not suited for skin lesion segmentation, because it is skewed towards the background. Thus we utilize the Jaccard distance as the loss function, which is more suitable for class imbalances. The results of the loss functions are shown in Table 3, with the Jaccard index providing the best results.

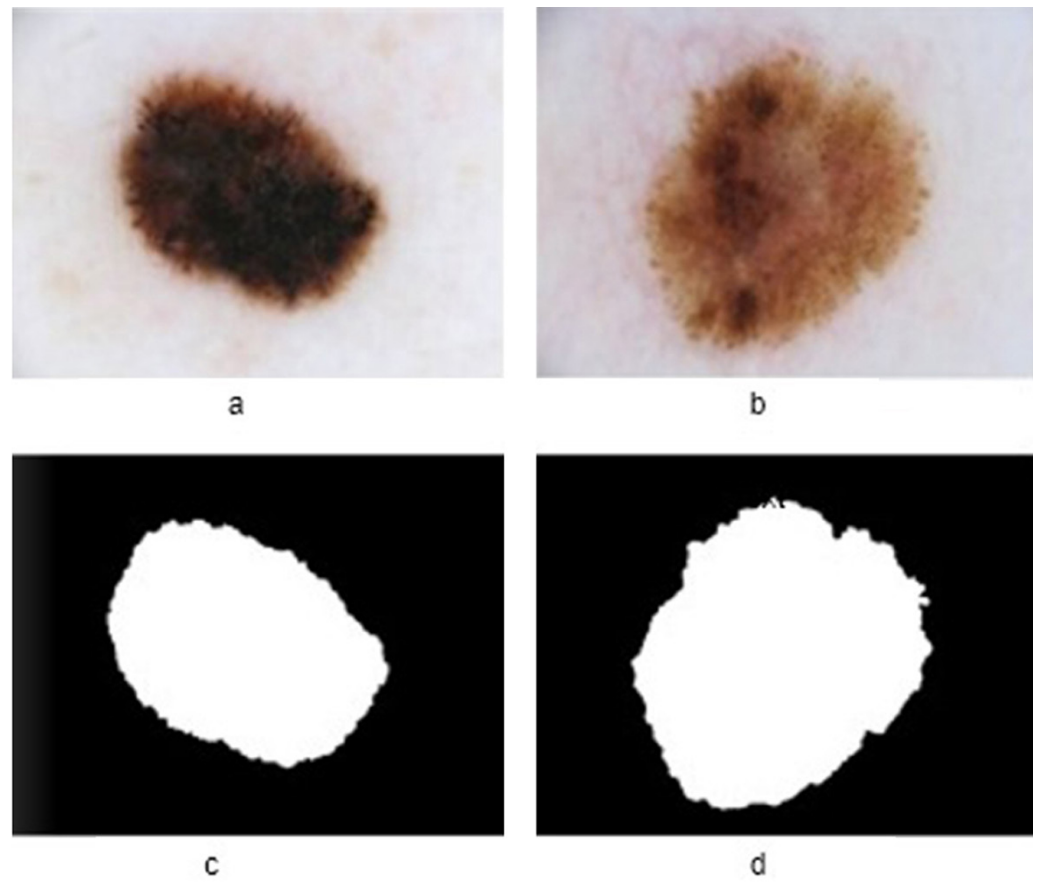


Fig. 5. Sample of segmented images obtained by our proposed model

Figure 5 shows a sample of the segmented outcome produced by the ResFCNET model. The images (a) and (b) represent the input images. Images (c) and (d) are the corresponding outputs.

Table 4. Comparison with other works

Input Size	Accuracy	Dice	Jaccard	Sensitivity	Specificity
Kolekar et al. [15]	0.928	0.845	0.928	0.889	0.948
Yu et al. [40]	0.949	0.897	0.829	0.911	0.957
Mahmudur et al. [51]	0.952	0.895	0.822	0.880	0.969
Our study	0.971	0.942	0.866	0.925	0.989

4.2 Comparison with other deep learning algorithms

Tables 4 and 5 presents a comparison of our model with other deep learning models fitted on the same dataset with the same number of epochs after running 65 epochs with each model, showing Accuracy, Dice, Jaccard, Sensitivity and Specificity. When we look at Accuracy, for instance, 97.1% is higher than any other machine learning algorithm. It means deep learning gives the best ability to recognize skin lesion on the body as well as to provide the best overall performance. This result shows that our model was successful at segmenting skin lesion.

Table 5. Comparison with similar models

Model	Accuracy	Dice	Jaccard	Sensitivity	Specificity
CNN	0.953	0.910	0.843	0.910	0.965
Inception V3	0.949	0.897	0.829	0.911	0.957
VGG16	0.952	0.895	0.822	0.880	0.969
ResFCNET	0.971	0.942	0.866	0.925	0.989

5 DISCUSSION

This study was aimed at supporting the efficient analysis of dermoscopic data to aid the automatic diagnosis and detection of melanoma, deemed to be the deadliest form of skin cancer. After running 150 epochs on the ResFCNET model, as well as established models such as CNN, Inception V3, and VGG16, Accuracy, Dice, Jaccard, sensitivity, and specificity were recorded. Our accuracy of 97.1% is higher than any of the compared state-of-the-art models. Again, the Jaccard similarity index of 86.6% obtained by our model is very high compared with the existing models. The model was evaluated on multiple evaluation metrics, as shown in Tables 4 and 5, allayed any doubt about the performance of our model. This performance means that the ResFCNET deep neural network model gives the best ability to recognize skin lesion on the body as well as providing the best overall performance.

Additionally, the introduction of residual network, a recent variation of convolutional neural network for reading dermoscopic images and perform visual detection and recognition in this study, is a novelty in the research. This approach provided a great result and can provide a pathway for skin specialists to apply deep learning to augment their human expertise in the field.

6 CONCLUSIONS

Skin lesions from dermoscopy data should be effectively segregated in order to achieve accurate skin cancer diagnosis. In this paper, a deep learning method based on a residual and full convolutional neural network named ResFCNET was proposed to perform semantic segmentation of skin lesions. In all, our model achieves an average Jaccard index of 85.5% on the ISBI 2016 skin lesion dataset and 86.6% on ISBI 2017 skin lesion dataset, respectively. The introduction of feature reuse in ResFCNET brings up new insights to further research in skin lesion recognition and forms the basis for future work. Future studies might want to explore larger amounts of datasets to reduce the likelihood of overfitting and increase performance of models. The successful comparative experimentation with other existing deep learning algorithms proves that our model is feasible. It also proves that the performance of deep learning methods in skin lesion recognition is better compared to machine learning-based approaches recently reported in the works of Noel et al. [52].

7 REFERENCES

- [1] S. Majumder and M. A. Ullah, "Feature extraction from dermoscopy images for an effective diagnosis of melanoma skin cancer," in *2018 10th International Conference on Electrical and Computer Engineering (ICECE)*, pp. 185–188, 2018. <https://doi.org/10.1109/ICECE.2018.8636712>

- [2] A. Adegun and S. Viriri, "Deep learning techniques for skin lesion analysis and melanoma cancer detection: a survey of state-of-the-art," *Artif. Intell. Rev.*, vol. 54, no. 2, pp. 811–841, 2021. <https://doi.org/10.1007/s10462-020-09865-y>
- [3] Z. Fu, J. An, Q. Yang, H. Yuan, Y. Sun, and H. Ebrahimian, "Skin cancer detection using Kernel Fuzzy C-means and Developed Red Fox Optimization algorithm," *Biomed. Signal Process. Control*, vol. 71, p. 103160, 2022. <https://doi.org/10.1016/j.bspc.2021.103160>
- [4] A. Zakaria, N. K. Howard, and B. K. Nkansah, "On the detection of influential outliers in linear regression analysis," *American Journal of Theoretical and Applied Statistics*, Vol. 3, no. 4, pp. 100–106, July 2014. <https://doi.org/10.11648/j.ajtas.20140304.14>
- [5] R. L. Siegel, K. D. Miller, and A. Jemal, "Cancer statistics, 2016," *CA. Cancer J. Clin.*, vol. 66, no. 1, pp. 7–30, 2016. <https://doi.org/10.3322/caac.21332>
- [6] F. K. Nezhadian and S. Rashidi, "Melanoma skin cancer detection using color and new texture features," in *2017 Artificial Intelligence and Signal Processing Conference (AISP)*, pp. 1–5, 2017. <https://doi.org/10.1109/AISP.2017.8324108>
- [7] F. Nachbar *et al.*, "The ABCD rule of dermatoscopy: high prospective value in the diagnosis of doubtful melanocytic skin lesions," *J. Am. Acad. Dermatol.*, vol. 30, no. 4, pp. 551–559, 1994.
- [8] K. Thurnhofer-Hemsi, E. López-Rubio, E. Domínguez, D. A. Elizondo, F. K. Nezhadian, and S. Rashidi, "Melanoma skin cancer detection using color and new texture features," *2017 Artif. Intell. Signal Process. Conf.*, vol. 9, pp. 1–5, 2017.
- [9] P. Tschandl, C. Rosendahl, and H. Kittler, "The HAM10000 dataset, a large collection of multi-source dermatoscopic images of common pigmented skin lesions," *Scientific Data*, vol. 5, p. 180161, 2018. <https://doi.org/10.1038/sdata.2018.161>
- [10] R. Gu, L. Wang, and L. Zhang, "DE-Net: A deep edge network with boundary information for automatic skin lesion segmentation," *Neurocomputing*, vol. 468, pp. 71–84, 2022. <https://doi.org/10.1016/j.neucom.2021.10.017>
- [11] R. D. Seeja and A. Suresh, "Deep learning based skin lesion segmentation and classification of melanoma using support vector machine (SVM)," *Asian Pacific J. cancer Prev. APJCP*, vol. 20, no. 5, p. 1555, 2019. <https://doi.org/10.31557/APJCP.2019.20.5.1555>
- [12] T. Akram, M. A. Khan, M. Sharif, and M. Yasmin, "Skin lesion segmentation and recognition using multichannel saliency estimation and M-SVM on selected serially fused features," *J. Ambient Intell. Humaniz. Comput.*, pp. 1–20, 2018. <https://doi.org/10.1007/s12652-018-1051-5>
- [13] J. Long, E. Shelhamer, and T. Darrell, "Fully convolutional networks for semantic segmentation," in *Proceedings of the IEEE conference on computer vision and pattern recognition*, pp. 3431–3440, 2015. <https://doi.org/10.1109/CVPR.2015.7298965>
- [14] S. Hong, H. Noh, and B. Han, "Decoupled deep neural network for semi-supervised semantic segmentation," *Adv. Neural Inf. Process. Syst.*, vol. 28, 2015.
- [15] S. S. Kolekar and P. G. Magdum, "Skin lesion semantic segmentation using convolutional encoder decoder architecture," in *2018 Fourth International Conference on Computing Communication Control and Automation (ICCUBEA)*, pp. 1–3, 2018. <https://doi.org/10.1109/ICCUBEA.2018.8697510>
- [16] R. Kaur, H. GholamHosseini, and R. Sinha, "Automatic Lesion Segmentation Using Atrous Convolutional Deep Neural Networks in Dermoscopic Skin Cancer Images," 2021. <https://doi.org/10.21203/rs.3.rs-285138/v1>
- [17] N. C. F. Codella *et al.*, "Deep learning ensembles for melanoma recognition in dermoscopy images," *IBM J. Res. Dev.*, vol. 61, no. 4/5, pp. 1–5, 2017. <https://doi.org/10.1147/JRD.2017.2708299>
- [18] J. S. Henning *et al.*, "The CASH (color, architecture, symmetry, and homogeneity) algorithm for dermoscopy," *J. Am. Acad. Dermatol.*, vol. 56, no. 1, pp. 45–52, 2007. <https://doi.org/10.1016/j.jaad.2006.09.003>

- [19] J. Gachon *et al.*, “First prospective study of the recognition process of melanoma in dermatological practice,” *Arch. Dermatol.*, vol. 141, no. 4, pp. 434–438, 2005. <https://doi.org/10.1001/archderm.141.4.434>
- [20] S. W. Menzies, “A method for the diagnosis of primary cutaneous melanoma using surface microscopy,” *Dermatol. Clin.*, vol. 19, no. 2, pp. 299–305, 2001. [https://doi.org/10.1016/S0733-8635\(05\)70267-9](https://doi.org/10.1016/S0733-8635(05)70267-9)
- [21] G. Argenziano *et al.*, “Seven-point checklist of dermoscopy revisited,” *Br. J. Dermatol.*, vol. 164, no. 4, pp. 785–790, 2011. <https://doi.org/10.1111/j.1365-2133.2010.10194.x>
- [22] M. Silveira *et al.*, “Comparison of segmentation methods for melanoma diagnosis in dermoscopy images,” *IEEE J. Sel. Top. Signal Process.*, vol. 3, no. 1, pp. 35–45, 2009. <https://doi.org/10.1109/JSTSP.2008.2011119>
- [23] Z. Ma and J. M. R. S. Tavares, “A novel approach to segment skin lesions in dermoscopic images based on a deformable model,” *IEEE J. Biomed. Heal. Informatics*, vol. 20, no. 2, pp. 615–623, 2015. <https://doi.org/10.1109/JBHI.2015.2390032>
- [24] D. D. Gómez, C. Butakoff, B. K. Ersboll, and W. Stoecker, “Independent histogram pursuit for segmentation of skin lesions,” *IEEE Trans. Biomed. Eng.*, vol. 55, no. 1, pp. 157–161, 2007. <https://doi.org/10.1109/TBME.2007.910651>
- [25] N. Z. Tajeddin and B. M. Asl, “A general algorithm for automatic lesion segmentation in dermoscopy images,” in *2016 23rd Iranian Conference on Biomedical Engineering and 2016 1st International Iranian Conference on Biomedical Engineering (ICBME)*, 2016, pp. 134–139. <https://doi.org/10.1109/ICBME.2016.7890944>
- [26] A. Pennisi, D. D. Bloisi, D. Nardi, A. R. Giampetruzzi, C. Mondino, and A. Facchiano, “Skin lesion image segmentation using Delaunay Triangulation for melanoma detection,” *Comput. Med. Imaging Graph.*, vol. 52, pp. 89–103, 2016. <https://doi.org/10.1016/j.compmedimag.2016.05.002>
- [27] L. Bi, J. Kim, E. Ahn, D. Feng, and M. Fulham, “Automated skin lesion segmentation via image-wise supervised learning and multi-scale superpixel based cellular automata,” in *2016 IEEE 13th International Symposium on Biomedical Imaging (ISBI)*, 2016, pp. 1059–1062. <https://doi.org/10.1109/ISBI.2016.7493448>
- [28] B. Bozorgtabar, M. Abedini, and R. Garnavi, “Sparse coding based skin lesion segmentation using dynamic rule-based refinement,” in *International Workshop on Machine Learning in Medical Imaging*, pp. 254–261, 2016. https://doi.org/10.1007/978-3-319-47157-0_31
- [29] A. Krizhevsky, I. Sutskever, and G. E. Hinton, “Imagenet classification with deep convolutional neural networks,” in *Advances in Neural Information Processing Systems*, pp. 1097–1105, 2012.
- [30] K. H. Cha, L. Hadjiiski, R. K. Samala, H.-P. Chan, E. M. Caoili, and R. H. Cohan, “Urinary bladder segmentation in CT urography using deep-learning convolutional neural network and level sets,” *Med. Phys.*, vol. 43, no. 4, pp. 1882–1896, 2016. <https://doi.org/10.1118/1.4944498>
- [31] D. C. Cireşan, A. Giusti, L. M. Gambardella, and J. Schmidhuber, “Mitosis detection in breast cancer histology images with deep neural networks,” in *International Conference on Medical Image Computing and Computer-assisted Intervention*, pp. 411–418, 2013. https://doi.org/10.1007/978-3-642-40763-5_51
- [32] Q. Dou *et al.*, “Automatic detection of cerebral microbleeds from MR images via 3D convolutional neural networks,” *IEEE Trans. Med. Imaging*, vol. 35, no. 5, pp. 1182–1195, 2016. <https://doi.org/10.1109/TMI.2016.2528129>
- [33] S. Miao, Z. J. Wang, and R. Liao, “A CNN regression approach for real-time 2D/3D registration,” *IEEE Trans. Med. Imaging*, vol. 35, no. 5, pp. 1352–1363, 2016. <https://doi.org/10.1109/TMI.2016.2521800>
- [34] A. Esteva *et al.*, “Dermatologist-level classification of skin cancer with deep neural networks,” *Nature*, vol. 542, no. 7639, p. 115, 2017. <https://doi.org/10.1038/nature21056>

- [35] S. Pereira, A. Pinto, V. Alves, and C. A. Silva, "Brain tumor segmentation using convolutional neural networks in MRI images," *IEEE Trans. Med. Imaging*, vol. 35, no. 5, pp. 1240–1251, 2016. <https://doi.org/10.1109/TMI.2016.2538465>
- [36] H. Alkahtani and T. H. H. Aldhyani, "Botnet attack detection by using CNN-LSTM model for internet of things applications," *Secur. Commun. Networks*, vol. 2021, 2021. <https://doi.org/10.1155/2021/3806459>
- [37] O. Ronneberger, P. Fischer, and T. Brox, "U-net: Convolutional networks for biomedical image segmentation," in *International Conference on Medical Image Computing and Computer-Assisted Intervention*, pp. 234–241, 2015. https://doi.org/10.1007/978-3-319-24574-4_28
- [38] L. Wang, L. Wang, H. Lu, P. Zhang, and X. Ruan, "Saliency detection with recurrent fully convolutional networks," in *European conference on Computer Vision*, pp. 825–841, 2016. https://doi.org/10.1007/978-3-319-46493-0_50
- [39] Y. LeCun, Y. Bengio, and G. Hinton, "Deep learning," *Nature*, vol. 521, no. 7553, p. 436, 2015. <https://doi.org/10.1038/nature14539>
- [40] L. Yu, H. Chen, Q. Dou, J. Qin, and P.-A. Heng, "Automated melanoma recognition in dermoscopy images via very deep residual networks," *IEEE Trans. Med. Imaging*, vol. 36, no. 4, pp. 994–1004, 2016. <https://doi.org/10.1109/TMI.2016.2642839>
- [41] M. H. Jafari, E. Nasr-Esfahani, N. Karimi, S. M. R. Soroushmehr, S. Samavi, and K. Najarian, "Extraction of skin lesions from non-dermoscopic images for surgical excision of melanoma," *Int. J. Comput. Assist. Radiol. Surg.*, vol. 12, no. 6, pp. 1021–1030, 2017. <https://doi.org/10.1007/s11548-017-1567-8>
- [42] D. Gutman *et al.*, "Skin lesion analysis toward melanoma detection: A challenge at the international symposium on biomedical imaging (ISBI) 2016, hosted by the international skin imaging collaboration (ISIC)," *arXiv Prepr. arXiv1605.01397*, 2016.
- [43] Y. Yuan, M. Chao, and Y.-C. Lo, "Automatic skin lesion segmentation using deep fully convolutional networks with jaccard distance," *IEEE Trans. Med. Imaging*, vol. 36, no. 9, pp. 1876–1886, 2017. <https://doi.org/10.1109/TMI.2017.2695227>
- [44] J. Zhang, C. Petitjean, and S. Ainouz, "Kappa loss for skin lesion segmentation in fully convolutional network," in *2020 IEEE 17th International Symposium on Biomedical Imaging (ISBI)*, pp. 2001–2004, 2020. <https://doi.org/10.1109/ISBI45749.2020.9098404>
- [45] K. He, X. Zhang, S. Ren, and J. Sun, "Deep residual learning for image recognition," in *Proceedings of the IEEE conference on computer vision and pattern recognition*, pp. 770–778, 2016. <https://doi.org/10.1109/CVPR.2016.90>
- [46] F. Chollet and others, "keras. GitHub repository," <https://github.com/fchollet/keras> Accessed on, vol. 25, p. 2017, 2015.
- [47] M. Abadi *et al.*, "Tensorflow: A system for large-scale machine learning," *12th USENIX Symposium on Operating Systems Design and Implementation (OSDI '16)*, pp. 265–283, 2016.
- [48] X. Glorot and Y. Bengio, "Understanding the difficulty of training deep feedforward neural networks," in *Proceedings of the Thirteenth International Conference on Artificial Intelligence and Statistics*, pp. 249–256, 2010.
- [49] L. Bottou, "Stochastic gradient descent tricks," in *Neural networks: Tricks of the trade*, Springer, pp. 421–436, 2012. https://doi.org/10.1007/978-3-642-35289-8_25
- [50] D. P. Kingma and J. Ba, "Adam: A method for stochastic optimization," *arXiv Prepr. arXiv1412.6980*, 2014.
- [51] M. MAHMUDUR RAHMAN, B. C. DESAI, and P. BHATTACHARYA, "Supervised machine learning based medical image annotation and retrieval in ImageCLEFmed 2005," *Lect. notes Comput. Sci.*, pp. 692–701, 2006. https://doi.org/10.1007/11878773_76
- [52] M. A. Al-Masni, D. H. Kim, and T. S. Kim, "Multiple skin lesions diagnostics via integrated deep convolutional networks for segmentation and classification," *Computer Methods and Programs in Biomedicine*, 190, p. 105351, 2020. <https://doi.org/10.1016/j.cmpb.2020.105351>

8 AUTHORS

Mustapha Adamu Mohammed, Department of Computer Science, Koforidua Technical University, Koforidua, Ghana. Department of Computer Science, Kwame Nkrumah University of Science and Technology, Kumasi, Ghana.

Obeng Bismark, School of Computer and Information Engineering, Zhejiang Gongshang University, Hangzhou, People's Republic of China.

Seth Alornyo, Department of Computer Science, Koforidua Technical University, Koforidua, Ghana.

Michael Asante, Department of Computer Science, Kwame Nkrumah University of Science and Technology, Kumasi, Ghana.

Bernard Obo Essah, Department of Statistics & Actuarial Science, University of Ghana, Legon-Accra, Ghana.